International Journal of Engineering Applied Sciences and Technology, 2022
Vol. 7, Issue 3, ISSN No. 2455-2143, Pages 316-320
Published Online July 2022 in IJEAST (http://www.ijeast.com)

ROBUSTNESS OF NTC-ALGORITHM FOR MISFITS IN CASE OF AIRFLOW CALIBRATION

Jan-Eric Kettner
EIT-Department
Hochschule Darmstadt, Darmstadt Germany

***Abstract*—Study with comparison of three-point airflow-auto calibration algorithm for NTC-thermistors. The results show that Hoge-5 is the best implementation of the NTC as well as the most robust to unavoidable calibration errors.**

Keywords—airflow, auto-calibration, automotive sensors, calibration, Hoge-1, Hoge-5, industrial environment, NTC, Steinhart-Hart, three-point calibration

I. INTRODUCTION

NTCs and similar thermo sensitive elements are widely used in industrial products like consumer electronics, IoT-devices, ventilating/air-conditioning systems in vehicles and residential spaces. The practical application of the thermo sensitive elements including the NTC have enabled the implementation of efficient energy saving methodologies.

Efficient energy control is quite important and can be shown for instance in the automotive industry. Smart air-conditioning of the passengers compartment is essential for lowering fuel consumption or extending the mileage of electric vehicles (Fritz et al., 2015; Wise J.A., 1992).

Heating, ventilation, and air conditioning systems (HVAC) consumes around 40 % of the total energy for passenger convenience systems in the modern vehicles. Therefore, real time & precise physical air parameter information including temperature and humidity measurement data become more relevant for designing an energy efficient system. (Fritz et al., 2015; Köppe et al., 2015)

The practical application of NTC (Bosson et al., 1950) or thermo sensitive elements as sensors will need calibration to gain when in use (Chung and Oh, 2015; Vaughn et al., 2006; Vaughn, 2012). The conventional and most followed thermistor calibration methodology includes a fluid tank with stirrer (Liu et al., 2018b, 2018a) , which has excellent heat distribution. However, the method mentioned above for calibration of thermistor is impractical in actual industrial settings. This is both due to only few of the components used for building the thermistor system are being sensitive to the fluid and due to the sheer volume of the sensors. An alternative method to calibrate the sensors is using a temperature chamber. This method has its own drawbacks, for example the temperature in such a chamber is not uniformly distributed therefore leading to errors in the calibrated sensors. Smart sensors allow the calibration of the thermistors efficiently. A smart sensor consists of an MCU (micro controller unit)(Figure 1) and a voltage divider comprising a NTC and a series resistor. The method employed in this case comprises also the use of a climate chamber for calibration.

During the sensor calibration process the microcontroller unit (MCU) calculates the required value based on the defined mathematical equation from the voltage divider (0.1)-(1.3). Both the values for the NTC and the series resistor R_S (with standard tolerance $\pm R$) are stored in a nonvolatile memory.

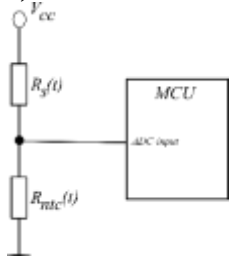

Figure 1 Schematics of MCU and temperature sensitive voltage divider

$$R_S = R_{nom.25°C} \pm R \quad (1.1)$$

$$R_S(T) = (R_{nom.25°C} \pm R) * (1 + \alpha \Delta T + \beta \Delta T^2 + \gamma T^3) \quad (1.2)$$

$$Val_{ADC}(t) = \frac{R_{NTC}(t)}{R_{NTC}(t) + R_s(t)} \quad (1.3)$$

A satisfying trade-off between process cost and sensor accuracy could be achieved by employing three-point calibration methods. Implementation of other curve fitting methods with more than three points, like polynomial regression, would result in an increase of process time and cost associated and therefore are not favorable for industrial production scenarios. On the other hand the implementation of simple two point calibrations would causes more inaccuracy as explained in the literature (Ilić et al., 2008).

A. NTC-Equations

There are different ways for describing the characteristics of NTC-thermistors. Steinhart-Hart (2.1) or Hoge-1 (2.2) with their individual coefficients (A_0, A_1, A_2) or Hoge-5 (2.3)

International Journal of Engineering Applied Sciences and Technology, 2022
Vol. 7, Issue 3, ISSN No. 2455-2143, Pages 316-320
Published Online July 2022 in IJEAST (http://www.ijeast.com)

and the coefficients (C_0, C_1, C_2) are the most common equations(Steinhart and Hart, 1968) used.

$$\frac{1}{T} = A_0 + A_1 \ln(R) + A_2 \ln(R)^3 \quad (2.1)$$

$$\frac{1}{T} = A_0 + A_1 \ln(R) + A_2 \ln(R)^2 \quad (2.2)$$

$$\frac{1}{T} = \frac{C_1 + C_2 \ln(R_t)}{1_1 + C_3 \ln(R_t)} \quad (2.3)$$

Numerous scientific studies have explored the effects of uncertainty during thermistor calibrations in fluid baths (Rudtsch and Rohden, 2015; Liu et al., 2018b). The outcome of these studies show that there is need for further examination of the problem associated with inaccurate NTC-thermistor calibration in temperature chambers. Furthermore, it is pointed out that using a rugged algorithm might be an essential part in finding the errors during calibration process by identifying non-uniformly distributed temperatures.

Our study can be divided into two stages. The first stage of the study includes the simulation which is based on the data available from the dataset. The second stage focuses on real data acquisition, including sensor measurements using approximations of various NTC-characteristics. These measurements are performed in the temperature chamber. By comparing the results of the stage 1 and stage 2 afterwards it is expected to give more insight to the nature of calibration errors and how to avoid them.

A. Simulation with NTC data

As part of stage one a numerical simulation is performed with data available out of the datasheet[7]. From the available data a mathematical model is created and simulated along with a voltage divider circuit to evaluate the performance. Together with the numerical simulation the virtual calibration is performed by using calculated ADC Values at -15°C, 30°C and 50°C. Over the course of the simulation the ADC and the reference temperature (+/-0.1 K) were altered/varied in the scale of +/- 1, 2, 3 Digits for ADC and +/-0.1 K for reference temperatures. Based on the mathematical formulas (1.1, 1.2, and 1.3) Steinhart-Hart, Hoge-1 and Hoge-5 curve parameters were formulated. From the curve parameters the temperature values are derived in accordance with Ohizumi NSS4103 G34NTC [7] datasheet in one Kelvin steps. For each point in the numerical simulation a failure value was calculated. The square error sum (2.4)for each case is cumulated over k calculated temperature points and compared with individual cases.

$$\varepsilon_s^2 = \sum_{n=0}^{k} (t_{calc} - t_{data})^2 \quad (2.4)$$

B. Measurements in temperature chamber

In this part of the study, 44 physical sensors systems are calibrated and measured in a Weiss WT3-180-40 temperature chamber (Figure 2) (last calibrated in February 2019).
After approaching a temperature point and a settling time of one hour. the NTCs are measured. From the selected 44 sensors, half of the sensors are assembled with double values series resistance for examination on series resistor effects. Based on the mathematical formulas ((2.1),(2.2),(2.3)) Steinhart-Hart, Hoge-1 and Hoge-5 curve parameters were formulated and corresponding temperature values for the 44 test sensors were calculated.

Figure 2 Temperate chamber

The reference temperature over the test period is measured and calibrated using a Prema-3040 precision thermometer (calibration date February 2019) with a measurement uncertainty (tolerance) of 0.02K. The sensor calibration and the measurement process were controlled and monitored by means of a personal computer and a specialized engineering interface based on a LIN-automotive standard for data acquisition. Each sensor is measured twenty times at each temperature point.

Table 1 Test points for stage two

Test number	Measurement point in Degree Celsius °C
1	-38
2	-35
3	-30
4	-25
5	-20
6	-15
7	-10
8	-5

International Journal of Engineering Applied Sciences and Technology, 2022
Vol. 7, Issue 3, ISSN No. 2455-2143, Pages 316-320
Published Online July 2022 in IJEAST (http://www.ijeast.com)

9	0
10	15
11	20
12	25
13	30
14	35
15	40
16	45
17	50
18	55
19	60
20	70
21	75
22	80

II. RESULTS AND DISCUSSION

In this section of the paper results of the study are summarized and main findings of the work are discussed. The analysis of the sensor data is performed with Matlab®. Simulation with NTC-characteristic from datasheet-Stage 1

A. Simulation with NTC-characteristic from datasheet-Stage 1

Each algorithm has its own characteristic pole which is visible for Hoge-1 and Steinhart-Hart at the calibration points and for Hoge-5 at 25°C. As a result the poles for Steinhart-Hart and Hoge-1 (Figure 4-Figure 6) are caused from missing gradient from one calibration point to its neighbor (Figure 3). For this reason, no equation parameter can be calculated in this case

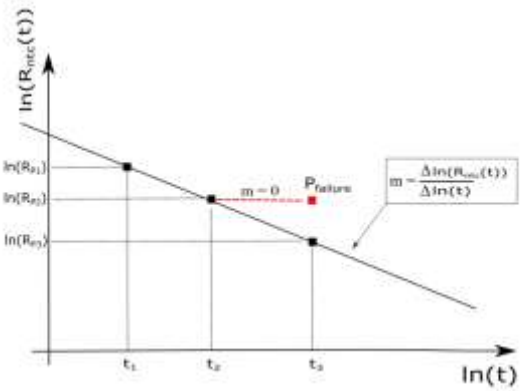

Figure 3 Explanation of calibration misfit in cause of no gradient between calibration points

Steinhart-Hart (Figure 4) shows a lot of calculation misfits. At higher temperatures the error gets more significant. Increase of the series resistor causes also higher errors. The Hoge-5 algorithm shows only one pole at the nominal point of 298,15 K (25°C) (Figure 6).

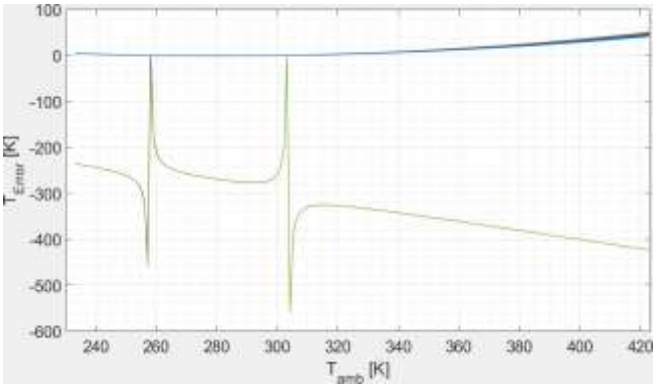

Figure 4 Exemplarily Steinhart-Hart simulation with correct parameters and missfitted curves with characteristical poles.

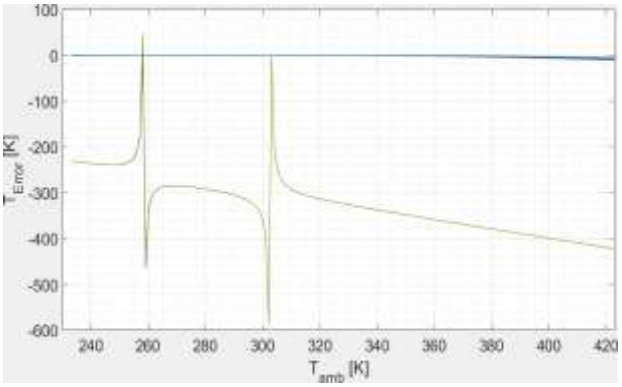

Figure 5 Exemplarily Hoge-1 simulation with correct parameters and, missfitted curves with characteristical poles.

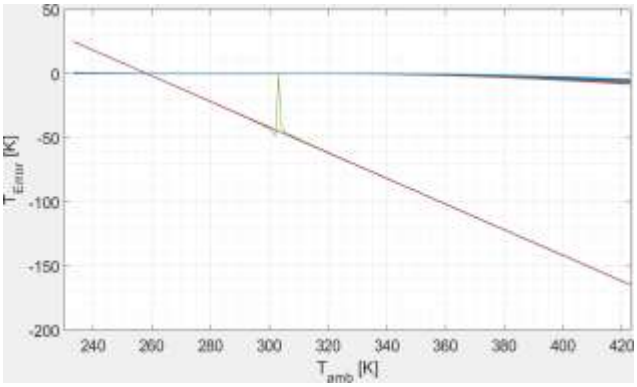

Figure 6 Exemplarily Hoge-5 simulation with correct parameters, missfitted curves with characteristical poles and curves with high error caused by miscalibration.

B. Temperature chamber results-Stage 2

Objective of this section is the evaluation of the calibration and measurement analysis for the physical sensors. Using Steinhart-Hart equation with high series resistance R_S for the sensors causes smaller deviations at low temperatures. Considering the middle range of test temperatures values, a left skewed deviation of temperature errors at low

temperatures can be observed due to response of the higher series resistance R_S value. If a low series resistance R_S is used the deviations at low temperatures tend towards right skewed, respectively in interval three-sigma. The errors of both variation in the middle values of the temperature in the test were approximately equal.

With Hoge-1 equation and low series resistance R_S deviations at high temperatures, errors were equal distributed at low temperatures towards left skewed. When series resistance R_S is high the errors at low temperatures were right skewed and they were left skewed at high temperatures in the three-sigma interval. For the middle values of temperature, the error distribution was equal.

Use of Hoge-5 as calculation algorithm with low series resistance R_S resulted in an equal distribution of the error in the three-sigma range. With high series resistor the error increased respectively at higher and lower temperatures. The deviation is observed in the case of low temperatures towards right skewed and at high temperatures left skewed. Error decreases to negative values for high temperatures were visible over the study.

In all cases errors decreases at higher temperature levels above the highest calibration temperature heavily due to negative errors. In the middle range of temperature values the errors are almost equal. The calculated square error sums (Table 2) shows that the most robust algorithm in relation miscalibration is Hoge-5. The results from the algorithm Steinhart-Hart resulted in lots of outliers above and under the calibrated range from -15°C to 50°C. Hoge-1 proved to be much better than Steinhart-Hart from the analysis of the study.

Table 2 calculated square errors for measured data in temperature chamber

EQUATION	$R_S \sim \frac{1}{2} R_{NTC}(25°C)$	$R_S \sim R_{NTC}(25°C)$
HOGE-1	**8.2865**	**14.3181**
HOGE-5	**7.2556**	**12.3449**
STEINHART-HART	**934.3281**	**1.0106e+03**

III. CONCLUSION

The study shows high level calibration methodology of the NTC. Most relevant finding of this study points to the fact that Hoge-5 algorithm proved to be the most robust algorithm in case of calibration errors, when three-point calibration is used.
A good value of the series resistor for the measuring tasks, is half value of the NTC resistor.

The results cannot be claimed universally for all NTC-calibrations done in air flow cambers. Future work includes the improvement on the means of airflow during the calibration process. The disabling or mixing of the flow with additional elements will also is imparted as future work.

THANKS
The authors gratefully acknowledge the support received from all branches ofsitronic GmbH & Co. KG.

IV. REFERENCE

[1] B. Corona, M. Nakano, H. Pérez, “Adaptive Watermarking Algorithm for Binary Image Watermarks”, Lecture Notes in Computer Science,Springer, pp. 207-215, 2004.

[2] A. A. Reddy and B. N. Chatterji, "A new wavelet based logo-watermarking scheme," Pattern Recognition Letters, vol. 26, pp. 1019-1027, 2005.

[3] P. S. Huang, C. S. Chiang, C. P. Chang, and T. M. Tu, "Robust spatial watermarking technique for colour images via direct saturation adjustment," Vision, Image and Signal Processing, IEE Proceedings -, vol. 152, pp. 561-574, 2005.

[4] F. Gonzalez and J. Hernandez, " A tutorial on Digital Watermarking ", In IEEE annual Carnahan conference on security technology, Spain, 1999.

[5] D. Kunder, "Multi-resolution Digital Watermarking Algorithms and Implications for Multimedia Signals", Ph.D. thesis, university of Toronto, Canada, 2001.

[6] J. Eggers, J. Su and B. Girod," Robustness of a Blind Image Watermarking Scheme", Proc. IEEE Int. Conf. on Image Proc., Vancouver, 2000.

[7] Barni M., Bartolini F., Piva A., Multichannel watermarking of color images, IEEE Transaction on Circuits and Systems of Video Technology 12(3) (2002) 142-156.

[8] Kundur D., Hatzinakos D., Towards robust logo watermarking using multiresolution image fusion, IEEE Transcations on Multimedia 6 (2004) 185-197.

[9] C.S. Lu, H.Y.M Liao, “Multipurpose watermarking for image authentication and protection,” IEEE Transaction on Image Processing, vol. 10, pp. 1579-1592, Oct. 2001.

[10] L. Ghouti, A. Bouridane, M.K. Ibrahim, and S. Boussakta, “Digital image watermarking using balanced multiwavelets”, IEEE Trans. Signal Process., 2006, Vol. 54, No. 4, pp. 1519-1536.

[11] P. Tay and J. Havlicek, "Image Watermarking Using Wavelets", in Proceedings of the 2002 IEEE, pp. II.258 – II.261, 2002.

[12] P. Kumswat, Ki. Attakitmongcol and A. Striaew, "A New Approach for Optimization in Image Watermarking by Using Genetic Algorithms", IEEE

Transactions on Signal Processing, Vol. 53, No. 12, pp. 4707-4719, December, 2005.

[13] H. Daren, L. Jifuen,H. Jiwu, and L. Hongmei, "A DWT-Based Image Watermarking Algorithm", in Proceedings of the IEEE International Conferenceon Multimedia and Expo, pp. 429-432, 2001.

[14] C. Hsu and J. Wu, "Multi-resolution Watermarking for Digital Images", IEEETransactions on Circuits and Systems- II, Vol. 45, No. 8, pp. 1097-1101, August 1998.

[15] R. Mehul, "Discrete Wavelet Transform Based Multiple Watermarking Scheme", in Proceedings ofthe 2003 IEEE TENCON, pp. 935-938, 2003.